UNIVERSITY OF NIŠ
The scientific journal **FACTA UNIVERSITATIS**
Series: **Working and Living Environmental Protection** Vol. 1, No 4, 1999, pp. 19 - 25
Editor of series: Ljiljana Rašković, e-mail: ral@junis.ni.ac.yu
Address: Univerzitetski trg 2, 18000 Niš,YU, Tel. +381 18 547-095, Fax: +381 18 547-950
http:// ni.ac.yu/Facta

MODELING OF SIDE - SCAN SONAR FIELD

UDC 534.873

Tihomir Trifonov[1], Yassen Siderov[2], Kamen Simenov[3]

[1]Vassil Levski Land Forces Academy, Faculty of Communication and Information Systems, Dep. of Radioelectronics, 5007 Veliko Turnovo, Bulgaria,
[2]University of Veliko Turnovo "St. st. Cyril and Methodius", Fac. of Mathematics and Informatics, 5003 Veliko Turnovo, Bulgaria
[3]P.O. Box 341, 5000 Veliko turnovo, Bulgaria

Abstract. *Analytical and experimental results of side-scan sonar field are presented. Nearfield and far-field simulation programs are used. A simple technique for measuring the width of the directivity pattern in an acoustic tank is offered.*

Key words: *side-scan sonar, antenna system, directivity pattern*

1. INDTRODUCTION

The creation of the side-scan sonars (SSS) in 1958 is a crucial point in the designing of technical devices for visualization of underwater objects, especially of objects near the sea bottom. The image obtained by SSS is in the usual for humans orthoscopic projection with much better resolution ability than the known by now have [1,2,3].

By these reasons different types SSS are widely used not for civil purposes only, but in military domain for detection and localization of objects on the sea floor or near it: wrecks, sea-bottom pipelines, mine belts etc.

One of the most significant systems of the SSS is the antenna system (transducer arrays). The main parameters of the sonar depend to a great extend on its optimal design and measurement [4].

2. OBSERVATION METHOD

The observation method is schematically shown in Fig. 1. The tow-fish is moved with a constant speed on a determined altitude above the sea bottom *h*. The image of the two

Received July 26, 1999

side bands is obtained up to the distrance $r_{\max}$.

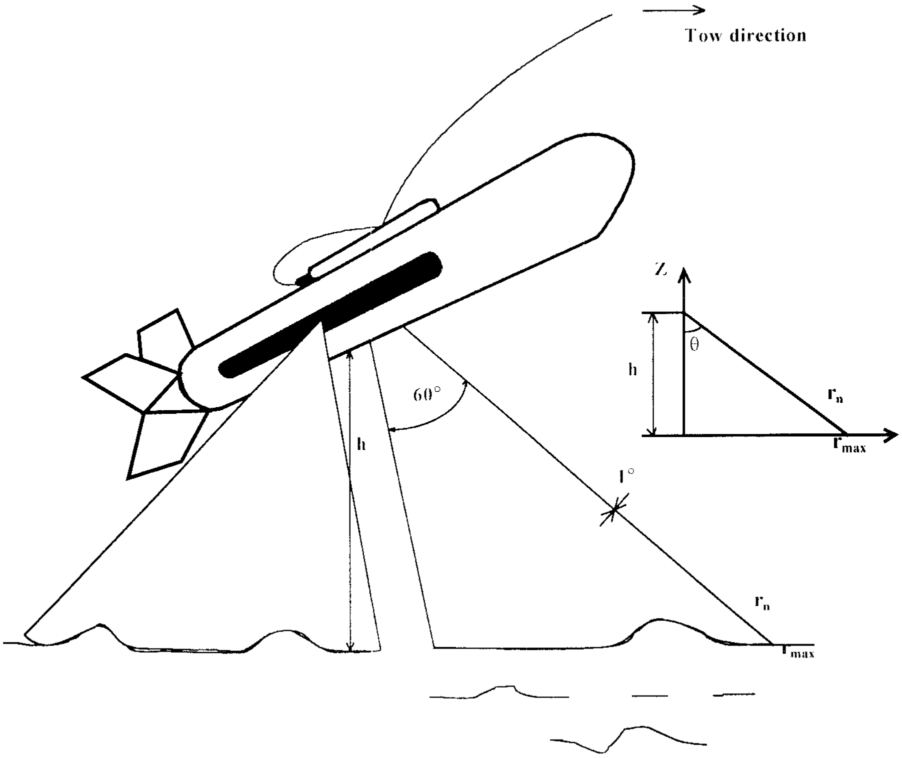

Fig. 1.

Under the condition that r_n/h is too big, it can be accepted thar $r_{\max}$ is equal to the slope distance r_n. The investigation, taking place at Radio-Technical Equipment Institute - Veliko Turnovo showed that the optimal relation is:

$$\frac{r_n}{h} \approx 8 \tag{1}$$

The width of the directivity pattern (DP) for each antenna in the azimuthal plane is about 1^0, and in the vertical one - about 60^0, and it can be recommended its form to satisfy the requirement [1]:

$$R(\theta) = \left(\frac{\cos ec\theta}{\sec \theta_{\max}} \right)^{\frac{3}{2}} \tag{2}$$

This DP provides steadiness of the investigated band radiation.

The indication of the sea floor, together with the adjacent sound-reflecting objects is realized in Cartesian coordinates "slope distance - tow distance". The information is memorized periodically on TV type indicators or electonic-chemical recorders, using electrochemical paper.

3. ANTENNA SYSTEM FIELD MODELING

Besause of the big directivity of the antennas in azimuthal (horizontal) plane, their main parameters can be obtained by approximation with the discrete linear antenna grid and can be measured by simple method, described below [4].

This problem is more complicated in the vertical plane. In this case it can be assumed that DP is formed by a pulsing strip, Build on an absolutely rigid in acoustical sense cylinder - Fig. 2.

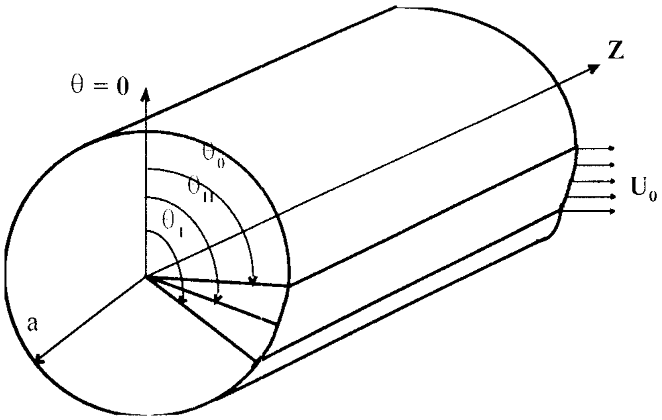

Fig. 2.

The general solution of the Helmholtz equation for a two-dimensional boundary-value problem (no dependence on "z" coordinate) is as follows [5]:

$$\Phi(r,\theta)=\sum_{m=0}^{\infty}(C_m\cos m\theta+D_m\sin m\theta)[E_mJ_m(kr)+F_mN_{m(kr)}] \tag{3}$$

where $J_m(kr)$ and $N_m(kr)$ - Bessel functions of the first and second kind m-th order
$\Phi(r,\theta)$ - field potential.

In order to satisfy the Sommerfeld condition, Fm=i. Em is assumed and then:

$$\Phi(r,\theta)=\sum_{m=0}^{\infty}(C_m\cos m\theta+D_m\sin m\theta)H_m^{(1)}(kr) \tag{4}$$

where $H_m^{(1)}(kr)$ is Bessel function of the third kind m-th order (also called the first Hankel function).

In the case shown in Fig. 2, the velocity of vibration depends on the angle θ by low $U_a = U_0(\theta)$ and in (4) it can be seoarated the solutions that satisfy the boundary condition (5) only:

$$U_0=-k\sum_{m=0}^{\infty}H_m^{(1)}(ka)(C_m\cos m\theta+D_m\sin m\theta) \tag{5}$$

If (5) is considered as Fourier Series, it can be obtained:

$$C_0 = -\frac{1}{2k\pi h_0^{(1)}(ka)} \int_{\alpha}^{\alpha+2\pi} U_0(\theta) d\theta\,; \tag{6}$$

$$C_m = -\frac{1}{k\pi H_m^{(1)}(ka)} \int_{\alpha}^{\alpha+2\pi} U_0(\theta)\cos m\theta d\theta\,; \tag{7}$$

$$D_m = -\frac{1}{k\pi H_m^{(1)}(ka)} \int_{\alpha}^{\alpha+2\pi} U_0(\theta)\sin m\theta d\theta\,; \tag{8}$$

m = 1,2,3,...

k - wave number, $k = \frac{2\pi}{\lambda}$

For this problem:

U_a = U_0, when $\theta \le \left|\frac{\theta_1 - \theta_0}{2}\right|$

U_a = 0, when $\theta > \left|\frac{\theta_1 - \theta_0}{2}\right|$

Solving (6,7,8) and substituting in (4), for the potential $\Phi(r,\theta)$ in the outside domain it can be written:

$$\Phi(r,\theta) = \frac{U_0}{2\pi k}(\theta_1 - \theta_0) \sum_{m=0}^{\infty} \frac{H_m^{(1)}(kr)}{\varepsilon_m H_m^{(1)}(kr)} \cos[m(\theta - \theta_n)] \tag{10}$$

where ε_m = 1, when $m \neq 0$

ε_m = 0, when $m = 0$

$\theta_n = \theta_0 + \frac{\theta_1 - \theta_0}{2}$

Using the known relation between the potential Φ and the sound pressure p for harmonic exicitation

$$p = p\left(\frac{\partial \Phi}{\partial t}\right) \tag{11}$$

where p - mass density of the medium and between the potential and the velocity of vibration $\vec{\upsilon}$

$$\vec{\upsilon} = -grad\Phi$$

it can be obtained all characteristics of the field, inclusively near-field and far-field DP.

4. NUMERICAL AND EXPERIMENTAL RESULTS AND CONCLUSION

The modeling was carried out in MATLAB-a widely used medium for scientific computation and visualization (See Appendix 1). The DPs were calculated for the following input data:

$$a = 0.1m\,,\quad \theta_n = \frac{11\pi}{8}\,,\quad \frac{\theta_{1-\theta_0}}{2} = \frac{\pi}{9}\,(i.e.\,20^0)\,,\quad k = \frac{2\pi}{\lambda} = 440$$

in a near $r = 2a$ and a far $r = 100\ a$ field.

These DPs are presented in Fig. 3 and Fig. 4.

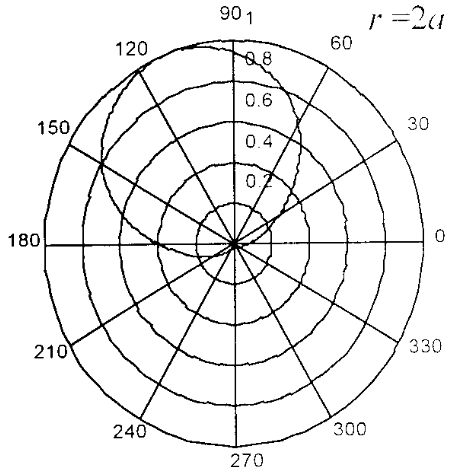

Fig. 3.

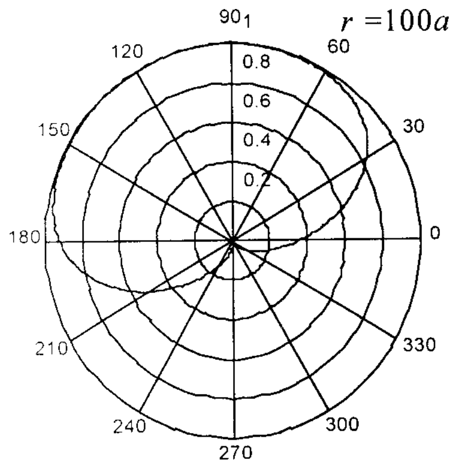

Fig. 4.

The complete results of testing show a good concidence with the measurement in the hydroacoustic measuring tank, in accordance with the current standards.

A simple method to the vertical coordinate device of the tank (Fig. 5).

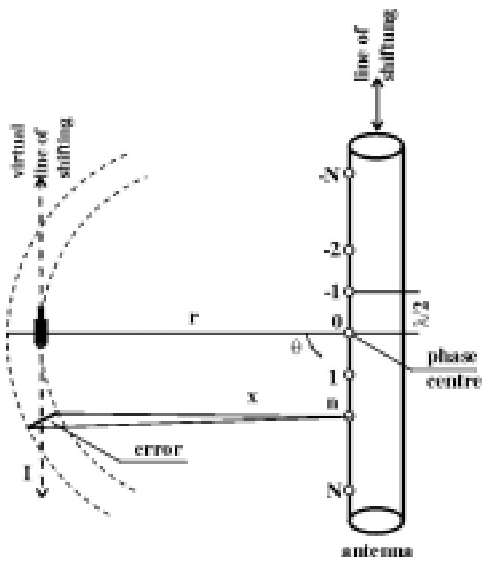

Fig. 5.

While shifting the antenna in the direction of its vertical axis, the level of the signal at the output of the measuring hydrophone is being watched. After reaching a certain level (e.g. 0.7 of the base maximum), linear shifting of the antenna in relation to the position of the main lobe of the DP is calculated by solving the obtained triangle. To evaluate the error, the continuous antenna is approximated with discrete with virtual element from *-N* to *+N*, with distance between them $\lambda/2$ [4]. The theoretical calculations are restricting the applicability of the method only in the near area of the main lobe of the DP, where the error is acceptable.

Conditions of a free field were created in a measuring tank: inner dimensions 14×7×7 m; sound-absorbing rubber panels;

sound-absorbing pontoons on the surface; vibroisolating foundations ensuring low level of the environmental noises; vertical thermal gradient lesser that 0.05 deg/m. The measurements were made with "Bruel&Kaer" measuring hydrophones and equimpent, using the impulse technique. The achieved relative error in measuring the width of the main lobe of the DP was only 1.5% hidher than the one, aditeved by using the classical method.

It's also important to mention, that the expences using the offered methods for modeling and DP measurement, are lesser that the ones expences made using the classical methods.

APPENDIX

```
% Program for calculation of
%Re P(r,tita)=-i.w.ro.Φ(r,tita)
% tita modifies from 0 to 360 %      degrees
format compact
ro=1000;             %kg/m^3 (density)
f=105*10^3; % frequency
w=2*pi*f;
k=440;
a=0.1;
r=100*a;
delta_tita=pi/9;
tita1=2*pi/3;
tita0=5*pi/9;
titaH=tita0+0.5*(tita1-tita0);
v0=1;
m=1;
while m ~= 8
m=menu('MENU','CALCULATION','new k', 'new a', 'new delta_tita', 'new tita0', 'new tita1', 'new v0', 'END');
 if m == 2
  disp(' ')
  disp(['the current value is: ' sprintf('%32.30f',k)])
  k=input('Enter new  k = ');
  while isnan(k)
   k=input('Enter   k = ');
  end
 end
 if m == 3
  disp(' ')
  disp([' the current value is: ' sprintf('%32.30f',a)])
  a=input('Enter new a = ');
  while isnan(a)
   a=input('Enter   a = ');
  end
  r=100*a
 end
 if m == 4
  disp(' ')
  disp(['the current angle is: ' sprintf('%32.30f',delta_tita) ' (' int2str(delta_tita*180/pi) ' degrees)'])
  delta_tita=input('Enter new  delta_tita = ');
  while isnan(delta_tita)
    delta_tita=input('Enter delta_tita = ');
  end
 end
 if m == 5
  disp(' ')
  disp(['the current angle is: ' sprintf('%32.30f',tita0) ' (' int2str(tita0*180/pi) ' degrees)'])
  tita0 = input('Enter new tita0 = ');
  while isnan(tita0)
   tita0=input('Enter tita0 = ');
  end
  titaH=tita0+0.5*(tita1-tita0)
  disp(['(' int2str(titaH*180/pi) ' degrees)'])
 end
 if m == 6
  disp(' ')
  disp(['the current angle is: ' sprintf('%32.30f',tita1) ' (' int2str(tita1*180/pi) ' degees)'])
tita0=input('Enter new   tita1 =');
  while isnan(tita1)
   tita1=input('Enter tita1=');
  end
  titaH=tita0+0.5*(tita1-tita0)
  disp(['(' int2str(titaH*180/pi) ' degrees)'])
 end
 if m == 7
  disp(' ')
  disp(['current value is: ' sprintf('%32.30f',v0)])
  v0=input('Enter        new v0=');
  while isnan(a)
   v0=input('Enter   v0 = ');
  end
 end

 if m == 1
  clc;
  t0=cputime;
  step_=pi/180;
p=zeros(1,round(360/step_));
  mm=0;
  for tita=0:step_:2*pi
  disp(['tita = ' sprintf('%18.15f',tita)
       ' (' int2str(tita*180/pi) ' degrees)'])
fi=firtita2(r,tita,v0,k,a,delta_tita,titaH);
  disp(['Φ(r,tita)=    ' sprintf('%18.15f',real(fi)) '+i*' sprintf('%18.15f',imag(fi))])
  mm=mm+1;
  p(mm)=-i*w*ro*fi;
  end
  sound(real(p),1111);
  disp(' ')
  disp(['Calculation time ' num2str(cputime-t0)     ' seconds'])
  disp('   PRESS A KEY')
  pause
  p=p/max(p);
  tita=0:step_:2*pi;
  hold on
% in cartesian coordinate
% system Real part
  ylabel('Re P');
  xlabel('tita [rad]');
  %      text(1,1,'DEKART; Real')
  real_p=real(p(1:mm));
  plot(tita,real_p)
% in cartesian coordinate
% system Abs
  figure
  ylabel('|P|');
  xlabel('tita [rad]');
  real_p=abs(p(1:mm));
  plot(tita,real_p)
  % in polar coordinates Real part
  figure
  real_p=real(p(1:mm));
  polar(tita,real_p)
% in polar coordinates Abs
  figure
  real_p=abs(p(1:mm));
  polar(tita,real_p)
 end % if m = 1
end % while m ~= 7
```

REFERENCES

1. A.V. Bogorodski, G.V. Yakovlev, E.A. Korepin, A.K. Doljikov, "Hydroacoustic Technology for Research and Exploitation of the Ocean", *Leningrad, Gidrometeoizdat, 1984, in Russian*
2. W.J. Zehner, R.L. Thompson, "Methods of Estimaiting Allowable Motion Perturbations in Side-Scan Sonar Systems", *IEEE Journal of Oceanic Engineering, Vol. 21. No. 3, July, 1996*
3. B. Stage, B. Zerr, "Detection of objects on the Sea Bottom Using Backscattering characteristics Depending on the Observation Point*", IEEE Journal of Ocean Engineering, Vol. 22, No. 1, January, 1997*
4. K.S. Simeonov, T.S. Trifonov, "Method for Directivity Pattern Measurements of Underwater Antennas", *Electronics and Electrotechnics, Vol. 33, No. 1-2, 1998, in Bulgarian*
5. E.L. Shenderov, "Wave Problems in Underwater Acoustics", *Leningrad, Sudostroenie, 1972*

MODELIRANJE POLJA SONARA SA BOČNIM SKENIRANJEM

Tihomir Trifonov, Yassen Siderov, Kamen Simeonov

Prezentirani su analitički i eksperimentalni rezultati polja sonara sa bočnim skeniranjem. Korišćeni su programi za simulaciju bliskog i dalekog polja. Nudi se prosta tehnika za merenje širine uzorka direktivnosti u akustičkim tankovima.